1-22-2002

Collision-Induced Electronic Energy Transfer From v=0 Of The E(0+g) Ion-Pair State In I2: Collisions With He And Ar

Christopher J. Fecko , '98

Miriam Arak Freedman , '00

Thomas Alex Stephenson
Swarthmore College, tstephe1@swarthmore.edu

Collision-induced electronic energy transfer from v=0 of the E(0 g +) ion-pair state in I 2 : Collisions with He and Ar

Christopher J. Fecko, Miriam A. Freedman, and Thomas A. Stephenson

Citation: The Journal of Chemical Physics **116**, 1361 (2002); doi: 10.1063/1.1427069
View online: http://dx.doi.org/10.1063/1.1427069
View Table of Contents: http://scitation.aip.org/content/aip/journal/jcp/116/4?ver=pdfcov
Published by the AIP Publishing

Collision-induced electronic energy transfer from $v=0$ of the $E(0_g^+)$ ion-pair state in I_2: Collisions with He and Ar

Christopher J. Fecko,[a] Miriam A. Freedman,[b] and Thomas A. Stephenson[c]
Department of Chemistry, Swarthmore College, Swarthmore, Pennsylvania 19081

(Received 20 August 2001; accepted 19 October 2001)

The electronic energy transfer pathways that occur following collisions between I_2 in the E ion-pair electronic state ($v=0$, $J=55$) and He and Ar atoms have been determined. The nearby D, D', and β ion-pair states are populated, but with relative branching ratios that vary with the rare gas collision partner. In He/I_2 collisions, the D state is preferentially populated, while Ar/I_2 collisions preferentially populate the β electronic state. Bimolecular rate constants and effective hard sphere collision cross sections have been determined for each channel; the cross sections range from 7.0 ± 1.0 Å^2 for populating the β state with Ar collisions to 0.9 ± 0.2 Å^2 for populating the D' state with He collisions. For both rare gas collision partners, and all three final electronic states, low vibrational levels are populated, in rough accord with the relevant Franck–Condon factors. There is little propensity observed for population of vibrational levels that are in near resonance with the initially prepared level in the E state. © *2002 American Institute of Physics.*
[DOI: 10.1063/1.1427069]

I. INTRODUCTION

A common outcome of a collision between an electronically excited diatomic molecule and a chemically inert collision partner is loss of some or all of the electronic energy from the diatomic species and translational, rotational, or vibrational excitation of the partner. Despite a number of detailed investigations, these collision-induced electronic energy transfer events remain inconsistently understood and highly system-dependent phenomena. In a recent review, Dagdigian has outlined the diversity of the experimental findings and the theoretical models that are used to describe them.[1] In general, models that provide good agreement for one particular system often fail for a different system, as the details of the intermolecular potential and/or the energy level structure of the collision partners are found to be crucial in modulating the electronic energy transfer dynamics.

Due to the relative ease of experimental investigation, the use of rare gas atoms and diatomic iodine in studies of inelastic collision dynamics has been extensive.[2–11] Specifically, the rotational and vibrational relaxation pathways that accompany collisions between rare gas atoms and electronically excited I_2 [in the $B(0_u^+)$ state] are perhaps the most extensively studied processes involving an electronically excited diatomic molecule. The electronic energy transfer processes that accompany such collisions have also been examined.[2,12–16] The information obtained has not been detailed, however, as the final state(s) populated in electronic energy transfer from the I_2 B state are invariably repulsive. Thus, while one can determine the overall cross section for collision-induced quenching, there is no opportunity to probe the nascent distribution of energy in the recoiling collision partners.

Common to all of the diatomic halogens is a set of more highly excited electronic states, the ion-pair states, which correlate with ionic halogen species. In I_2, the lowest energy tier of ion-pair states consists of six closely spaced, strongly bound ($D_e\approx31\,000\,\mathrm{cm}^{-1}$) electronic states, correlating with $I^+(^3P_2)+I^-(^1S_0)$.[17] In Fig. 1, we display the lowest energy portion of these six states, which carry the historical labels and Ω quantum numbers (in order of decreasing energy) $\delta(2_u)$,[18] $\gamma(1_u)$,[18] $E(0_g^+)$,[19] $D(0_u^+)$,[20,21] $\beta(1_g)$,[22] and $D'(2_g)$.[23] Note from the figure that the T_e values of these states all lie within 1500 cm^{-1} of one another, and that the R_e and ω_e values are quite similar.

The availability of six, closely spaced, bound, electronic states provides an opportunity for a detailed study of collision-induced electronic energy transfer that is difficult to reproduce in other systems. Indeed, there is rich history of such studies involving the ion-pair states in I_2. Typical experiments are those of Hemmati and Collins[24] and Martin *et al.*,[25] in which the $D\leftarrow X$ transition was excited using 193 nm photons, populating $v=132-134$ in the D state. By recording the I_2 wavelength-resolved emission spectrum with increasing buffer gas (Ar, N_2, or SF_6) pressure, these workers determined that the D state was quenched, and that a number of new emission features emerged. The most prominent of these was assigned to the D' state, though weaker emission from the E and F states were also observed. [The F state belongs to the next higher energy tier of ion-pair states, correlating with $I^+(^3P_0)+I^-(^1S_0)$.[17]] At low buffer gas pressures, the emission from the D' state was broad, suggesting that a large number of vibrational levels were populated.[25] With increasing pressure, the emission pattern

[a]Current address: Department of Chemistry, Massachusetts Institute of Technology, Cambridge, MA 02139.
[b]Current address: Department of Mathematics, University of Minnesota, Minneapolis, MN 55455.
[c]Author to whom correspondence should be addressed. Electronic mail: tstephel@swarthmore.edu

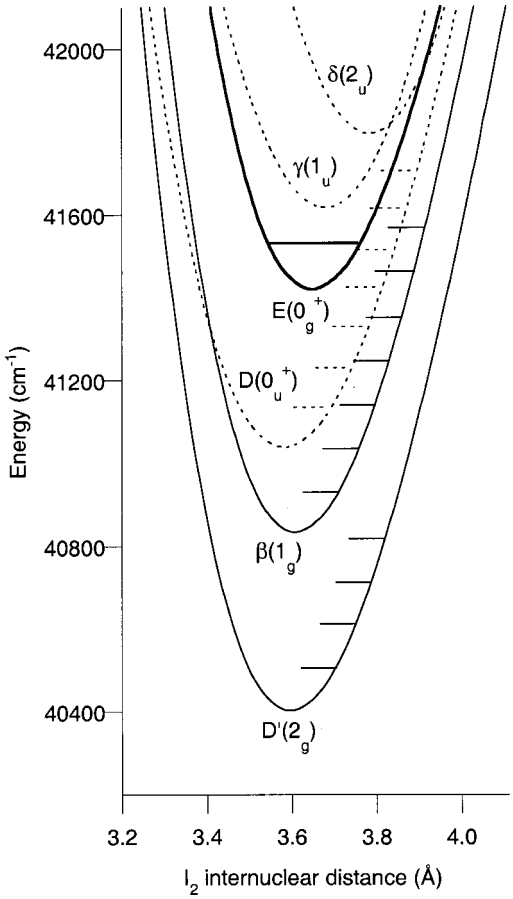

FIG. 1. The lowest tier of ion-pair electronic states in I_2. The *gerade* states are shown as solid lines; the *ungerade* states as dashed lines. This initially prepared level used in these studies, $v=0$ of the E state, is shown in bold. The energies of the vibrational levels in the D, β, and D' states populated by electronic energy transfer are indicated on the right of each potential energy curve.

narrows, as the D' state population was vibrationally relaxed. Similar results were found by Guy *et al.* for I_2 excited by a Tesla discharge in the presence of high pressures (200–700 Torr) of Ar.[26] In a more systematic pressure dependence study (1.7 to 378 Torr of Ar), Kvaran, Jonsdottir, and Thorgeirsson deduced that collision-induced electronic energy transfer was more efficient than vibrational relaxation following excitation of I_2 at 193 nm.[27] At the lowest Ar pressures, emission was observed from high vibrational levels of each of the ion-pair states. At intermediate pressures, vibrational relaxation became an important process within each vibrational manifold. In accord with earlier results, at high pressures, low vibrational levels of the D' state dominated as the populations became thermalized within this set of electronic states. The motivation for several of these studies was derived from the observation by Shaw *et al.* that upon excitation of I_2 at 193 nm, relaxation by Ar or SF_6 to the D' state was so efficient that laser action can be observed on the $D' \rightarrow A'$ transition at 342 nm.[28]

In a related experiment, Stephenson, Hong, and Lester excited the NeICl van der Waals complex to the β ion-pair state using a double resonance excitation scheme.[29] Dispersed emission spectra recorded following excitation of the complex revealed not only the expected vibrational predissociation, but also efficient and selective changes in the electronic state of the ICl. For example, upon excitation to $v=0$ in the β state, emission from the lower energy E and D' states was observed, with the branching ratio between these states dependent on the degree of excitation of the van der Waals stretching and bending vibrational coordinates. Excitation to higher vibrational levels resulted in emission from the D' and/or E states, with the branching ratio a sensitive function of the degree of ICl vibrational excitation.

More recently, Teule, Stolte, and Ubachs[30] and Akopyan *et al.*[31] reported on the $E \rightarrow D$ electronic energy transfer process that accompanied collisions between a number of atomic and diatomic species and $I_2(E)$. In these investigations, the collision partner pressures were lower than those reported previously, and single rotational levels were prepared in the E ion-pair state. When Teule, Stolte, and Ubachs prepared I_2 in the $v=8$, 13, and 15 levels of the E state and examined the D state emission that resulted from Ar/I_2 collisions, they found that near resonant energy transfer was preferred.[30] Akopyan *et al.* prepared a number of E state vibrational levels, $v=26-47$, and found that the distributions of vibrational energy in the D state were broad, particularly for Ar/I_2 collisions.[31] The roles of vibrational wave function overlap and vibrational energy gaps were critically examined as models for governing the disposition of vibrational energy in the electronic energy transfer process.

In a previous report from this laboratory, we have described the electronic energy transfer process that occurs when $I_2(E)$ collides with an $I_2(X)$ molecule.[32] We used an optical-optical double resonance excitation scheme to prepare single rotational levels in $v=0$ in the E ion-pair state. Briefly, we find that the D electronic state is populated exclusively, and that the vibrational distribution in the D state is dictated by a combination of energy gap and vibrational wave function overlap considerations. The cross section for this process is significant, 18 ± 3 Å^2. In the study described in the present paper, we extend this work by introducing Ar and He as collision partners. We consider the dynamics of a single rotational level, $J=55$ in $v=0$ in the E electronic state, and incorporate collision partner pressures that are lower than any of the previous investigations, assuring that single collision conditions are met. Our observations confirm that a variety of electronic energy transfer processes occur with rare-gas collision partners, and focus attention on our poor understanding of the relevant potential energy surfaces and the nonadiabatic dynamics that they support.

II. EXPERIMENT

The experimental strategy used in these investigations has been described in a previous publication from this laboratory.[32] Briefly, we prepare I_2 in a single rotational level ($J=55$) of the lowest vibrational level of the E ion-pair electronic state using two-color double resonance excitation. The initial $B \leftarrow X$ excitation occurs via the (20,0), $R(55)$ transition; the required 559.95-nm radiation is provided by a neodymium-doped yttrium aluminum garnet (Nd^{3+}:YAG) pumped dye laser (Continuum Lasers YG580-30/TDL-50) operating with Rhodamine 590 laser dye (Exciton). After a delay of 5–10 nanoseconds, the second photon excites a

fraction of the B state population using the $E \leftarrow B$ (0,20), $P(56)$ transition at 426.56 nm. This photon is provided by a N_2-pumped dye laser (Laser Photonics UV24/DL-14P) operating with Coumarin 440 laser dye (Exciton). Both lasers have a pulse width of 10 nanoseconds. The timing between the excitation lasers is controlled by a digital delay generator (Princeton Applied Research 9650 or Berkeley Nucleonics 555) and is variable over a wide range of delays. The emission features reported here occur only when the N_2 laser system fires coincident with or later than the YAG laser system; no emission is observed when one of the laser beams is blocked from reaching the sample chamber. The YAG-pumped dye laser operates with a spectral bandwidth of approximately 0.15 cm^{-1}; the bandwidth of the N_2-pumped dye laser is approximately 0.25 cm^{-1}.

Double resonance excitation of I_2 results in intense $E \rightarrow B$ emission between 415 and 435 nm, as well as a number of weaker features, depending on the sample pressure conditions. I_2 emission is collected by an $f/1.2$ fused silica optical system, and is focused onto the entrance slit of a 0.5-m focal length scanning monochromator (Instruments SA 500M). The monochromator is equipped with a 2400 groove/mm grating, providing a dispersion of 0.8 nm/mm. Typical slit widths are 100–200 μm. Wavelength resolved emission exiting the monochromator is detected by one of two methods. With the monochromator operating in scanning mode, emission is detected using a UV sensitive photomultiplier tube (Thorn/EMI 9613QB) mounted on the exit slit body. The output of the phototube is routed to a gated integrator (Stanford Research Systems SR250), with integrated emission intensities eventually stored on a laboratory computer using Labview software (National Instruments). Alternatively, the monochromator can operate as a spectrograph and a charge-coupled device (CCD) camera (Princeton Instruments LN/CCD-2500PB) replaces the exit slit body. Each of the 2500 pixel columns on the CCD chip is 12 μm wide, providing a total spectral coverage of 24 nm and a step size of 0.0096 nm.

I_2 vapor, at a pressure of 40 mTorr, and a variable pressure of either He or Ar, were held in a glass and fused silica cell, equipped with Brewster's angle laser inlet and exit windows. The cell was filled on a glass vacuum line pumped by a diffusion pump/mechanical pump combination to a base pressure of $\approx 2 \times 10^{-5}$ Torr. All pressures were measured with a capacitance manometer (MKS Baratron 127 series) with a precision of ± 1 mTorr. I_2 (Aldrich, 99.999%), He (MG, 99.9999%), and Ar (MG, 99.9995%) were used without additional purification.

Analysis of our emission spectra and the electronic energy transfer pathways required a number of Franck–Condon factors, which we calculated using the LEVEL program from Rydberg–Klein–Rees (RKR) potential energy curves.[33] We determined the RKR curves from the spectroscopic data provided in the literature for the E,[19] D',[23] and A (Ref. 34) states. We utilized directly the literature RKR curves for the D (Ref. 20), β (Ref. 22), A' (Ref. 35), and X (Ref. 36) states.

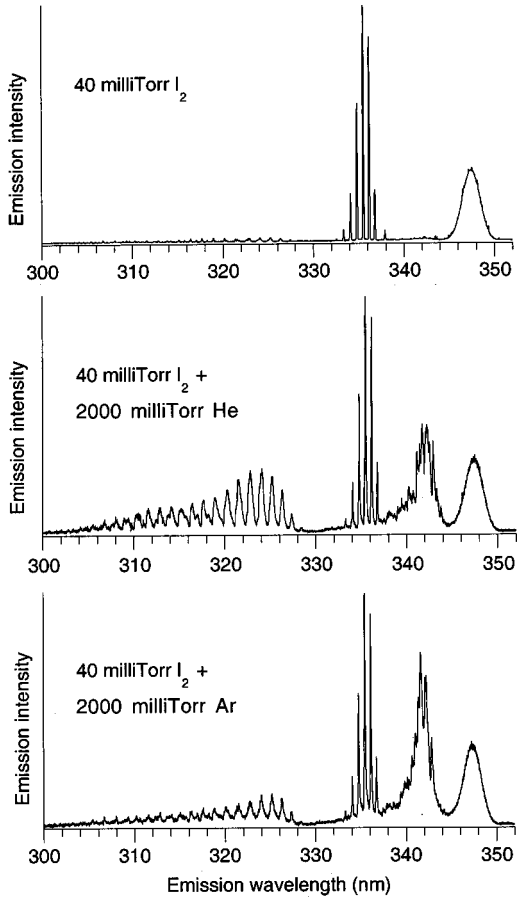

FIG. 2. Wavelength resolved emission spectra recorded following excitation of I_2 to the E ion-pair electronic state, $v=0$, $J=55$. Emission features are assigned to the following electronic band systems: 300–328 nm, $D \rightarrow X$; 333–338 nm, $E \rightarrow A$; 338–345 nm, $\beta \rightarrow A$ and $D' \rightarrow A'$; 345–350 nm, $E \rightarrow B''$.

III. RESULTS

In Fig. 2 (top), we display the ultraviolet portion of the emission spectrum recorded when 40 mTorr of I_2 is prepared in $J=55$ in the ground vibrational state of the E electronic state. The emission features centered at 335 and 348 nm are assigned to the well-studied $E \rightarrow A$ and $E \rightarrow B''$ transitions, respectively.[37] The weak emission beginning at 328 nm, and extending to shorter wavelengths, is assigned as $D \rightarrow X$ emission, with the D electronic state populated by collisions between $I_2(E)$ and $I_2(X)$ molecules. This process was the topic of a previous report from this laboratory.[32]

In the middle and bottom frames of Fig. 2 we show the changes that occur in the emission spectrum when He and Ar, respectively, are introduced into the sample cell. Qualitatively, the effects of the rare gases are the same: the $D \rightarrow X$ emission system becomes more intense, and a new feature, centered at $\approx$342 nm, appears. As discussed below, we assign this feature as a blend of the $\beta \rightarrow A$ and $D' \rightarrow A'$ emission systems. On closer examination, we note that differences between He and Ar exist, in that we observe a higher population of the D state when He is the collision partner, and a higher population of the β and D' states when $I_2(E)$ collides with Ar. We quantify both of these effects later in this section.

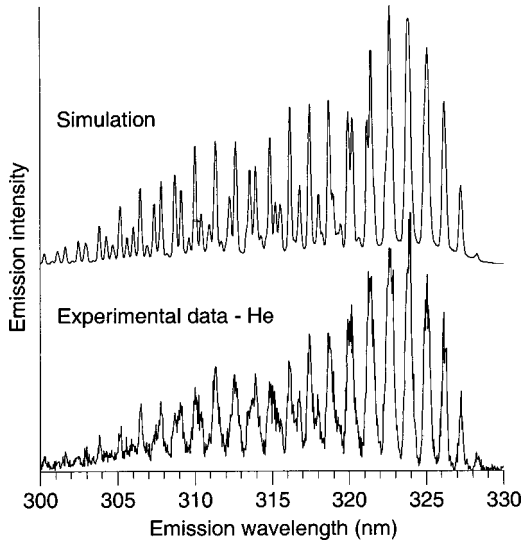

FIG. 3. Collision-induced $D \rightarrow X$ emission spectrum recorded following excitation to the E electronic state. The I_2 pressure is 40 mTorr, the He pressure is 750 mTorr.

A. Analysis of $D \rightarrow X$ spectra

We utilize a least-squares fit to the recorded $D \rightarrow X$ emission spectra to extract the collision-induced populations in the D state vibrational levels. In Figs. 3 and 4, we show an example of the emission spectra, and our best fit to the data, for He and Ar collision partners, respectively. In these fits, we treat the populations of the $v=0-7$ vibrational levels in the D electronic state as variable parameters and determine the best fit to the experimental spectra with a least squares routine. With ≈ 0.1 nm spectral resolution, we are unable to resolve rotational structure in these spectra. To account for the width of some of the features and the lack of baseline resolution between the features, we assume that a number of rotational levels are populated. As in our previous publication, we model this distribution by choosing a functional form frequently used in ro-vibrational energy transfer,[38] given by

$$P(J_f) = (2J_f + 1)\left(\frac{\Delta E_{\mathrm{rot}}}{B_v}\right)^{-\alpha},$$

where $P(J_f)$ is the probability of populating rotational level J_f, ΔE_{rot} is the change in the rotational energy of the molecule, B_v is the rotational constant for the D state vibrational level in question, and α is a parameter determined by the quality of fit to the experimental data. For collisions with He, we find that $\alpha = 0.65$ provides that best fit to the experimental spectrum, while we set $\alpha = 0.55$ for collisions with Ar. We lack sufficient resolution to quantitatively test the adequacy of this energy gap model for the rotational distribution, or to determine whether different values of α should be assigned to the different D state vibrational levels that we populate. We simply find this model to be a convenient means to introduce a distribution of rotational populations into our fitting procedure.

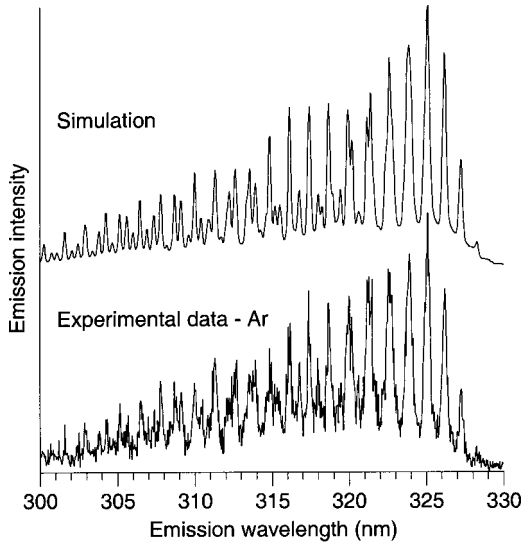

FIG. 4. Collision-induced $D \rightarrow X$ emission spectrum recorded following excitation to the E electronic state. The I_2 pressure is 40 mTorr; the Ar pressure is 1000 mTorr.

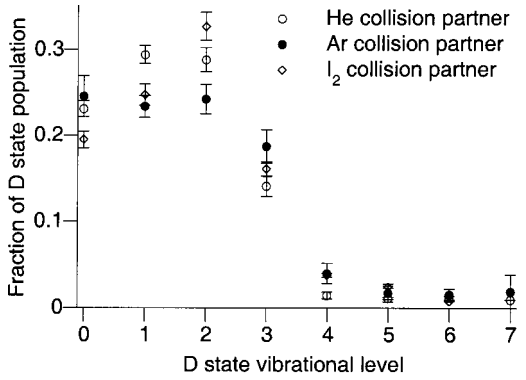

FIG. 5. D electronic vibrational distributions extracted from simulations of $D \rightarrow X$ emission spectra. The data on I_2/I_2 collisions are taken from Ref. 32.

In Fig. 5, we present the distribution of vibrational states populated in the D electronic state following collisions with He, Ar, and $I_2(X)$, with the last of these data drawn from Ref. 32. Note that, qualitatively, these distributions are quite similar. In each case, the lowest four vibrational levels account for more than 90% of the population. Regardless of the collision partner, we find that $v=1$ and 2 have populations that are comparable to (or larger than) $v=0$. When $I_2(X)$ is the collision partner, however, $v=2$ is the level with the highest population; this distinguishes I_2/I_2 collisions from those involving rare gas atoms. We will return to the significance of these results in the discussion.

Using a kinetic analysis, we can extract the bimolecular rate constants for the population of the D electronic state. We consider four possible processes, assuming single-collision conditions:

$$I_2(E) \rightarrow I_2(B,A,B'') + h\nu, \quad k_1$$

$$I_2(E) + \mathrm{He/Ar} \rightarrow I_2(D) + \mathrm{He/Ar}, \quad k_{\mathrm{RG}}$$

$$I_2(E) + I_2(X) \rightarrow I_2(D) + I_2(X), \quad k_X$$

$$I_2(D) \rightarrow I_2(X) + h\nu, \quad k_3.$$

TABLE I. Electronic energy transfer rate constants and effective hard-sphere collision cross sections.

Collision partner	Ion-pair state populated	Rate constant (10^{-17} m^3 s^{-1} molecule^{-1})	Effective hard-sphere collision cross section (Å^2)
$I_2(X)$	D	4.0±0.7[a]	18±3[a]
He	D	3.8±0.5	3.0±0.4
Ar	D	2.0±0.4	4.7±0.9
He	β	1.2±0.2	1.0±0.2
Ar	β	3.0±0.5	7.0±1.0
He	D'	1.1±0.2	0.9±0.2
Ar	D'	1.0±0.2	2.4±0.4

[a]Reference 32.

By integration of the differential rate equations that result from this kinetic scheme, we find

$$\frac{I_D}{I_E}=\frac{k_{\mathrm{RG}}[\mathrm{RG}]+k_X[\mathrm{I_2}(X)]}{k_1},$$

where I_D and I_E are the emission intensities from the D and E electronic states, respectively, and [RG] is the He or Ar concentration. The transition moments and emission lifetimes of all of the lowest tier ion-pair states have been measured by Lawley *et al.*[39] These data, when combined with our experimentally determined intensity ratios ($D\rightarrow X/E\rightarrow A$), allow us to determine the bimolecular rate constants for electronic energy transfer. (We account for the contribution of I_2/I_2 collisions to the $E\rightarrow D$ energy transfer using our previously published data.[32]) As summarized in Table I, the rate constant for $E\rightarrow D$ transfer is $(3.8\pm0.5)\times10^{-17}$ m^3 sec^{-1} molecule^{-1} when He is the collision partner and $(2.0\pm0.4)\times10^{-17}$ m^3 sec^{-1} molecule^{-1} when Ar is the collision partner. In Fig. 6, we show the linear dependence of the $D\rightarrow X$ emission signal on rare gas pressure; the rate constants quoted above are averaged over all rare gas pressures. The figure also demonstrates that the $D\rightarrow X$ emission signal is larger when He is the collision partner for all pressures, which is reflected in the larger bimolecular rate constant for this process. Also provided in Table I are the effective hard sphere collision cross sections for $E\rightarrow D$ electronic energy transfer, calculated by noting that $k=\sigma v$, where v is the mean relative velocity of the colliding species. For He/I_2 collisions, $v=1265$ m sec^{-1}, and for Ar/I_2 collisions, $v=428$ m sec^{-1}. This large difference in mean relative velocities results in an inverse trend in the collision cross sections, with electronic energy transfer with Ar having a σ value of 4.7±0.9 Å^2, while He has a smaller cross section, 3.0±0.4 Å^2. We note that both of these cross sections are smaller than that determined previously, 18±3.0 Å^2, for the $E\rightarrow D$ energy transfer that accompanies $I_2(E)/I_2(X)$ collisions.[32]

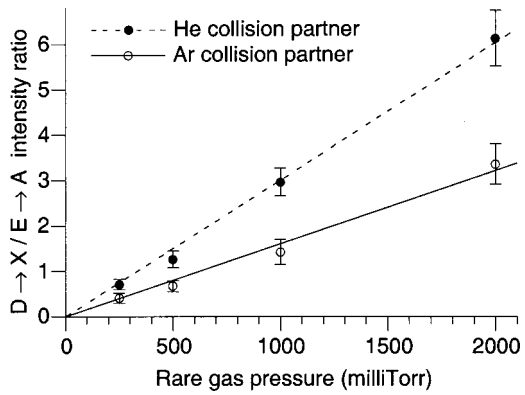

FIG. 6. Rare gas pressure dependence of the ratio of the $D\rightarrow X$ to $E\rightarrow A$ emission intensities. The lines represent the best linear fits through the origin.

We find that the vibrational state distributions presented in Fig. 5 are independent of rare gas pressure, over the range 250–2000 mTorr. This observation, combined with the linear pressure dependence shown in Fig. 6, strongly suggests that we have achieved single collision conditions. To quantify this assumption, we use the expression proposed by Yamasaki and Leone for the probability P_n, that a gas phase species undergoes n collisions in a time Δt,

$$P_n=\frac{1}{n!}\left(\frac{v\Delta t}{\lambda}\right)^n e^{-v\Delta t/\lambda},$$

where v is the mean relative velocity of the colliding species and λ is the mean free path.[40] For He/I_2 collisions at a He pressure of 2000 mTorr, we find that P_0, the probability of no collisions, is 0.735, while P_1, the probability of one collision is 0.226. The probability of more than one collision is $1-P_0-P_1$, which we determine to be 0.039. Thus of those I_2 molecules that experience one collision, 17% experience multiple collisions. At a He pressure of 250 mTorr, this figure drops to 2.6%. At all pressures, I_2 molecules experiencing single collisions outnumber those experiencing multiple collisions by more than 4.8:1.

B. Analysis of $\beta\rightarrow A$ and $D'\rightarrow A'$ spectra

In Fig. 7, we display spectra recorded at slightly longer emission wavelengths, showing features corresponding to the $\beta\rightarrow A$ and $D'\rightarrow A'$ transitions, as well as the $E\rightarrow A$ transition. Also shown in the figure are our fits to these spectra, obtained using the procedure described in the previous section. Because the vibronic transitions of the $\beta\rightarrow A$ and $D'\rightarrow A'$ systems overlap in the region between 338 and 344 nm, we have included both systems in our fits. Specifically, emission from $v=0-6$ in the β state and $v=0-3$ in the D' have been considered. Higher vibrational levels in the β state were found to lack statistically significant population in our fits, while higher vibrational levels in the D' state were excluded after examination of the Franck–Condon profiles of the resulting emission. For example, we found that emission from $v=4$ and higher in the D' state shows detectable Franck–Condon activity in the region between 332 and 335 nm. Since we do not observe any such features in our spectra, these vibrational levels were excluded from our fits. Based on our signal-to-noise ratio, we estimate that the contribution of $v\geqslant4$ in the D' state is less than 5% of the total population.

Comparison of the quality of the fits shown in Fig. 7 with those shown in Figs. 3 and 4 reveals that the β/D' state fits are significantly less satisfying. While the positions of the

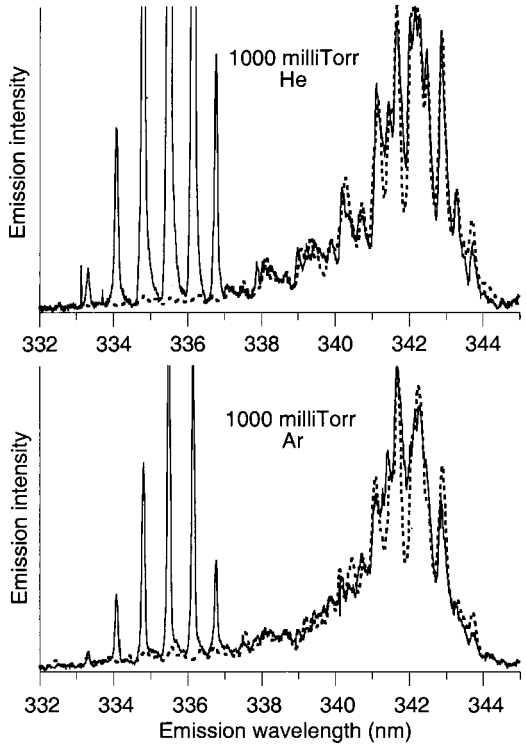

FIG. 7. $\beta \rightarrow A/D' \rightarrow A'$ emission spectra recorded following excitation of the E electronic state. The I_2 pressure is 40 mTorr; the rare gas pressure is 1000 mTorr for both spectra. The solid lines are the experimental data; the dashed lines are the simulations. The sharp features between 333 and 337 nm are the $E \rightarrow A$ transitions.

features are well reproduced in the fits, the intensities and, especially, the breadths of certain features are not well described. We attribute these shortcomings to deficiencies in the model for the distribution of rotational energies in the β and D' states. In both cases, we utilize the functional form described previously for emission from the D state. Lacking rotational resolution in our spectra, we have assumed that the distribution of rotational energy is the same for all vibrational levels in the β and D' states. We find that the best fits are achieved when $\alpha = 0.80$ for He collisions and $\alpha = 0.70$ for Ar collisions. The assumption of uniform rotational distributions is almost certainly incorrect, and our fits can be improved by adjusting the α parameters for different vibrational levels and electronic states. The extent of the overlap of the vibronic features is so severe, however, that any such analysis would not be unique. We have chosen, therefore, to retain the uniform distribution assumption because it implies the minimal amount of information about the actual rotational energy distribution, consistent with the lack of resolution of rotational structure in our experiments.

Also complicating our analysis of the collision-induced spectral features in this region is uncertainty concerning the presence of emission from the $\delta(2_u)$ ion-pair state. Bound-free emission from the δ state, centered at 342 nm, has been identified by Lawley *et al.*[39] The lower state is reported to be the uncharacterized 2_g repulsive state that correlates with two $^2P_{3/2}$ I atoms. Clearly, the spectral complexity of the region around 342 nm does not allow us to determine whether or not the δ state is appreciably populated in a

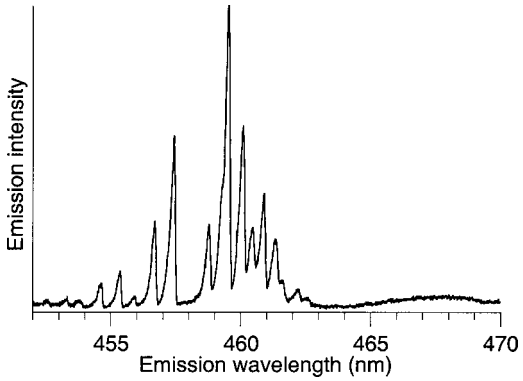

FIG. 8. Emission spectra showing $D \rightarrow 0_g^+$ transitions (454–463 nm) and possible $\delta \rightarrow 2_g$ bound-free transition at longer wavelength. The I_2 pressure is 40 mTorr, the He pressure is 2000 mTorr.

collision-induced process. (Note that the lowest vibrational level of the δ state lies 371 cm^{-1}, or $\approx 1.8kT$, above the energy of $v = 0$ in the E state, so this process is energetically feasible.) To clarify this issue, we have recorded a spectrum at longer wavelength, to search for the presence of a second bound-free transition originating in the δ state. Emission to a different repulsive 2_g state, this one correlating with $I(^2P_{3/2}) + I(^2P_{1/2})$, is reported to occur at $\approx$465 nm.[39] In Fig. 8, we show the results of this measurement, recorded with 2000 mTorr of He as collision partner. The discrete features observed between 453 and 463 nm can be readily assigned to $D \rightarrow 0_g^+$ vibronic transitions. This 0_g^+ state also correlates with one ground state and one spin-orbit excited I atom and has been characterized by Ishiwata *et al.*[41] Between 464 and 469 nm, we observe a weak continuous emission feature, that we cannot rule out as being a $\delta \rightarrow 2_g$ transition. Fortunately, Lawley *et al.* measured the transition moments for both $\delta \rightarrow 2_g$ transitions, at $\approx$342 and $\approx$465 nm.[39] Based on the intensity of the 464–469-nm feature, we have determined that δ state emission accounts for at most 10% of the spectral intensity between 338 and 344 nm. We consider even this minority contribution as being extremely unlikely, as the $\delta(v = 2) \rightarrow 2_g$ spectrum reported by Lawley *et al.* exhibits a maximum at 342.5 nm, and substantial emission intensity at 344 nm.[39] Between 342.5 and 344 nm, we can account for all of the observed spectral intensity by assuming that only the β and D' states are populated.

In Fig. 9, we display the β and D' state vibrational distributions obtained when He and Ar are the collision partners, while in Fig. 10 we show the rare gas pressure dependence of the β, D' emission intensity. Several aspects of these data are worthy of note. First, for both collision partners and both electronic states, the lowest vibrational level is populated. Second, as in the case of energy transfer to the D electronic state, the lowest vibrational levels ($v = 0-3$) account for a significant majority of the total population. Third, He and Ar behave differently as collision partners in terms of the branching between the β and D' states. Following He/I_2 collisions, approximately equal numbers of molecules populate the β and D' states. Following Ar/I_2 collisions, the β state population is larger than that of the D' state by a factor of 3. Fourth, Ar is clearly more efficient at inducing elec-

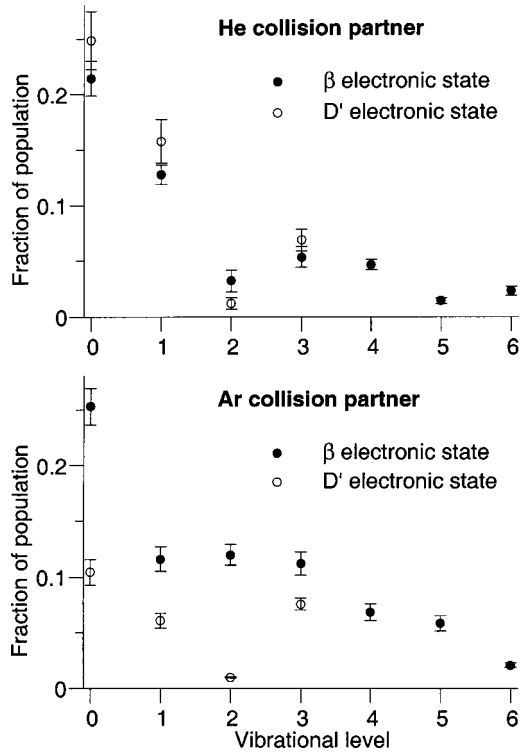

FIG. 9. β and D' state vibrational distributions extracted from spectral simulations when He (top panel) and Ar (lower panel) are the collision partners.

tronic energy transfer to the β and D' states than is He. This trend is quantified in Fig. 10 and in Table I, where we have listed the calculated rate constants and effective collision cross sections for all of the processes examined in this paper, along with the I_2/I_2 collision data presented previously. Examination of the trends in the rate constants/cross sections reveals that collisions between $I_2(E)$ and He are more likely to result in population in the D electronic state than either the β or D' states. On the other hand, collisions of $I_2(E)$ with Ar are more likely to result in population of the β state than either the D or D' states. The selectivity of the electronic energy transfer pathways is both surprising and significant.

Finally, the overall rate constants for electronic energy transfer are roughly comparable for He and Ar, $\approx 6 \times 10^{-17}\,m^3\,s^{-1}\,molecule^{-1}$. As noted previously, however, the difference in mean relative velocities between He/I_2 and Ar/I_2 collisions means that the overall cross section for electronic energy transfer with Ar collisions is approximately a factor of 3 larger than that for He collisions, 14.4 ± 2.4 and 4.9 ± 0.8 Å^2, respectively.

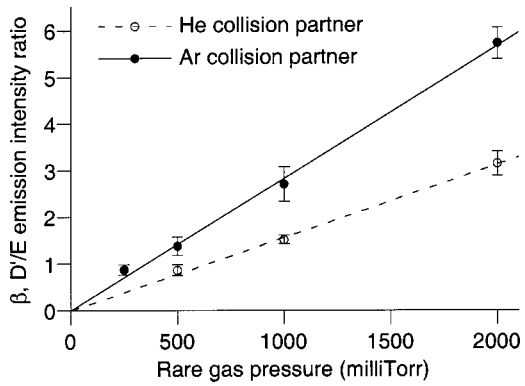

FIG. 10. Rare gas pressure dependence of the ratio of the $\beta \rightarrow A$ and $D' \rightarrow A'$ to $E \rightarrow A$ emission intensities. The lines represent the best linear fits through the origin.

TABLE II. Franck–Condon factors between the E ion-pair state, $v=0$, and vibrational levels of the D, β, and D' ion-pair states ($J=55$).

Vibrational level, v	$\lvert\langle E_{v=0} \rvert D_v\rangle\rvert^2$	$\lvert\langle E_{v=0} \rvert \beta_v\rangle\rvert^2$	$\lvert\langle E_{v=0} \rvert D'_v\rangle\rvert^2$
0	0.663	0.853	0.763
1	0.294	0.138	0.214
2	4.09×10^{-2}	8.62×10^{-2}	2.25×10^{-2}
3	1.94×10^{-3}	2.61×10^{-4}	1.12×10^{-3}
4	2.00×10^{-5}	4.06×10^{-6}	2.73×10^{-5}
5	1.82×10^{-10}	3.06×10^{-8}	3.26×10^{-7}
6	3.69×10^{-9}	4.08×10^{-10}	3.28×10^{-10}

IV. DISCUSSION

In Fig. 1, we display the potential energy curves for the ion-pair electronic states, along with the energies of the vibrational levels that we find populated following collision-induced electronic energy transfer. In our previous publication, we noted that the $E \rightarrow D$ energy transfer that accompanies collisions with $I_2(X)$ does not result in substantial population of the nearly resonant $v=4$ energy level in the D state ($\Delta E = -9\ cm^{-1}$).[32] This result is confirmed in the present study; we find that low vibrational states, with substantial energy gaps, are preferentially populated in all three electronic states by collisions with He and Ar. For example, all of the D' state vibrational levels populated have energy gaps greater than 700 cm^{-1}, and the most populated level, $v=0$, is 1020 cm^{-1} lower in energy than $v=0$ in the E state. Similarly, despite the presence of a β state level, $v=6$, with an energy gap of only 32 cm^{-1}, the most populated level is $v=0$, with an energy gap of 588 cm^{-1}. For all electronic states, and both rare-gas collision partners, we find that near resonant electronic energy transfer accounts for less than 5% of the total process. This result is identical to that observed previously in our study of $I_2(E)I_2(X)$ collisions.[32]

The large population observed in the lowest vibrational states is qualitatively in accord with the Franck–Condon theory for electronic energy transfer.[1] According to this model, the propensity for populating a particular vibrational state is linearly related to the square of the vibrational overlap integral between the initial and final vibrational states. In Table II, we list the Franck–Condon factors that link the ground vibrational level of the E state with the lowest seven vibrational levels of the D, β, and D' states. In each case, the $v=0$ level has the largest overlap with the initially prepared state, and the Franck–Condon factors decrease rapidly with increasing vibrational excitation. On a more quantitative level, we see that the Franck–Condon model provides an inexact description of the energy transfer process. In our previous report, we suggested that energy gap considerations may serve to modulate the effect of the Franck–Condon fac-

tors, such that the vibrational level populations decrease with v more gradually than the Franck–Condon factors, in general agreement with the data presented here.

An aspect of the vibrational distributions that is more difficult to understand is the qualitative difference between the D state distributions on one hand, and the β and D' state distributions on the other. Figure 5 demonstrates that the D state distributions are relatively insensitive to collision partner and that $v=0$, 1, and 2 all have substantial population. In contrast, in Fig. 9 we note that in the β and D' states, the distributions are sharply peaked at $v=0$, independent of the rare gas or the final electronic state. In our study of $I_2(E)/I_2(X)$ collisions, we suggested that the large populations in $v=1$ and 2 are due to a near resonance between the energy released upon population of these levels (291 and 197 cm^{-1}, respectively) and the spacing between $v=0$ and 1 in the $I_2(X)$ collision partner (213 cm^{-1}).[32] Clearly, the presence of substantial population in $v=1$ and 2 of the D state when the collision partner is a rare gas atom weakens this argument. We note, however, that while the populations in $v=0-2$ in the D state are, within experimental error, the same following collisions with Ar (and nearly so for He collisions), $v=2$ is more populated by a factor of 1.67 relative to $v=0$ following $I_2(X)$ collisions. Given that the energy released in populating $v=2$ is out of resonance with the X state vibrational spacing by only 16 cm^{-1}, vibrational excitation of the I_2 collision partner remains a viable explanation for the enhancement of $v\neq 0$ population in the D state with the diatomic collision partner. Our results using rare-gas collision partners clearly demonstrate, however, that this effect is not unique and may not even dominate the distribution of vibrational energy in $E\rightarrow D$ electronic energy transfer. Note that in Table II, the Franck–Condon factors for $E\rightarrow D$ energy transfer are less sharply peaked at $v=0$ than is the case for $E\rightarrow\beta$ or $E\rightarrow D'$ transfer. Based on this observation, one might expect greater population in $v=1$ in the D state than in the β or D' states, as observed. These simple trends fall apart, however, for $v=2$ and higher vibrational levels.

The small propensity for population of the near resonant vibrational levels in the D state is in contrast to the work of Teule, Stolte, and Ubachs, in which the energy gap effects appear to dominate the distribution of vibrational energy in the D state.[30] Teule, Stolte, and Ubachs prepared I_2 in higher vibrational levels of the E state, $v=8$, 13, and 15, and found that collisions with Ar resulted in preferential population of the nearest resonant D state vibrational level in all cases. For these higher vibrational levels, the Franck–Condon factors connecting the initially prepared level with the various D state levels observed vary by at most a factor of 100.[32] Table II demonstrates, however, that the $E-D$ Franck–Condon factors vary by as much as 10^8 for $v=0$ in the E state. A consistent interpretation of these data is that both Franck–Condon and energy gap effects are important, and that near resonant energy transfer occurs, as long as the relevant Franck–Condon factors are not too small. Larger energy gap pathways are substantially populated when the Franck–Condon effects favor them overwhelmingly.

$E\rightarrow D$ electronic energy transfer with He and Ar collision partners has also been observed by Akopyan *et al.*[31] In this work, high vibrational levels ($v=26-47$) of the E state are initially excited. He/I_2 collisions result in the loss of up to 320 cm^{-1} of vibronic energy, and the vibrational distributions qualitatively follow the trends in the Franck–Condon factors. When Ar is the collision partner, Akopyan *et al.* find a significantly broader vibrational distribution (up to 15 D states levels are populated), and note that vibrational levels up to 160 cm^{-1} higher in energy than the initial E state level are populated.[31] The peak of the distribution corresponds to vibrational levels with large Franck-Condon overlap with the initially prepared level, though not consistently the largest degree of vibrational overlap. These workers suggest a model for nonresonant electronic energy transfer that assumes that the interaction potentials between I_2 and a rare gas atom are somewhat different for $I_2(E)$ and $I_2(D)$. As a result, intermolecular surfaces correlating with D state levels with smaller overall vibronic energy intersect the intermolecular surface correlating with the initially prepared level. These surface crossings provide an opening for electronic energy transfer. Nothing in our data contradicts this intriguing model, but absent information on the details of the intermolecular potentials, it is impossible to confirm (or refute) the underlying principles. Akopyan *et al.* also observed emission from the D' and/or β states following collisions with He and Ar, but did not analyze the spectra due to lack of adequate spectral resolution.[31]

Our data show that the cross section for electronic energy transfer is approximately a factor of 3 times larger for Ar/I_2 collisions than for He/I_2. This trend is consistent with both physical intuition and previous studies of electronic energy transfer on species such as CN,[42] CO,[43] and N_2.[44,45] Of greater interest is the dependence of the electronic branching fractions on the rare gas collision partner. As noted in Table I, the relative cross sections for the population of the D, β, and D' states in He collisions are 0.64:0.19:0.17, while the same ratios are 0.33:0.50:0.17 for Ar/I_2 collisions. The origin of this effect is unclear. It is, however, similar to the anomalous branching fraction observed in collisions of rare gas atoms with CO in the $a\,^3\Pi$ state.[43] In this case, collisions with Ne, Ar, Kr, and Xe result in a relatively constant branching between the $a'\,^3\Sigma^+$ and $d\,^3\Delta$ electronic states. Collisions with He result, however, in disproportionate population in the $a'\,^3\Sigma^+$ state.[43] Similarly, the relative collision-induced couplings of the $B\,^2\Pi_g$ state in N_2 with the $A\,^3\Sigma_u^+$ and $W\,^3\Delta_u$ states exhibits a dependence on the rare gas species involved in the collision.[44] Both the CO and N_2 experiments utilize a beam/gas configuration, resulting in a variation in the mean center-of-mass collision energy with rare gas species.[43,44] It is not surprising, therefore, that the branching factors differ, as the collisions can access different portions of the intermolecular potential energy surface. Our experiments, however, occur under thermal equilibrium conditions, with constant mean center-of-mass collision energies. It is likely, therefore, that the different branching fractions are a reflection of the rare gas dependence of the intermolecular potentials, which surely differ for Ar and He. Specifically, we expect that the Ar/I_2 intermolecular potential is more attractive than that for He/I_2. This effect will also impact the positions of the repulsive walls of the potentials

correlating adiabatically with the I_2 ion-pair electronic states. Thus, we expect that the opportunity for differential nonadiabatic interactions will be abundant, even in the unlikely event that the intermolecular interactions are identical for each of the ion-pair states. If, in addition, there is a significant difference in the way, for example, that $I_2(D)$ and $I_2(\beta)$ interact with a rare gas atom, the possibility for rare gas dependent branching fractions are magnified even further. Unfortunately, we have very little knowledge of the potential energy surfaces that correlate with the I_2 ion-pair states. The data that we have presented should be a sensitive test for future computational models of the rare gas I_2 intermolecular potentials, and the scattering events that they support.

ACKNOWLEDGMENTS

This research has been supported by a grant from the National Science Foundation. One of the authors (T.A.S.) is grateful for the support of the Camille and Henry Dreyfus Foundation in the form of a Henry Dreyfus Teacher-Scholar Award (1994–1999).

[1] P. J. Dagdigian, Annu. Rev. Phys. Chem. **48**, 95 (1997).
[2] J. I. Steinfeld and W. Klemperer, J. Chem. Phys. **42**, 3475 (1965).
[3] R. B. Kurzel and J. I. Steinfeld, J. Chem. Phys. **53**, 3293 (1970).
[4] J. I. Steinfeld and A. N. Schweid, J. Chem. Phys. **53**, 3304 (1970).
[5] R. B. Kurzel, J. I. Steinfeld, D. A. Hatzenbuhler, and G. E. Leroi, J. Chem. Phys. **55**, 4822 (1971).
[6] D. J. Krajnovich, K. W. Butz, H. Du, and C. S. Parmenter, J. Chem. Phys. **91**, 7705 (1989).
[7] D. J. Krajnovich, K. W. Butz, H. Du, and C. S. Parmenter, J. Chem. Phys. **91**, 7725 (1989).
[8] H. Du, D. J. Krajnovich, and C. S. Parmenter, J. Phys. Chem. **95**, 2104 (1991).
[9] S. L. Dexheimer, M. Durand, T. A. Brunner, and D. E. Pritchard, J. Chem. Phys. **76**, 4996 (1982).
[10] S. L. Dexheimer, T. A. Brunner, and D. E. Pritchard, J. Chem. Phys. **79**, 5206 (1983).
[11] W. G. Lawrence, T. A. Marter, M. L. Nowlin, and M. C. Heaven, J. Chem. Phys. **106**, 127 (1997).
[12] J. E. Selwyn and J. I. Steinfeld, Chem. Phys. Lett. **4**, 217 (1969).
[13] G. A. Capelle and H. P. Broida, J. Chem. Phys. **58**, 4212 (1973).
[14] J. Derouard and N. Sadeghi, Chem. Phys. Lett. **102**, 324 (1983).
[15] U. K. A. Klein, J. Mastromarino, and A. Suwaiyan, Chem. Phys. Lett. **217**, 86 (1994).
[16] K. Nakagawa, M. Kitamura, K. Suzuki, T. Kondow, T. Munakata, and T. Kasuya, Chem. Phys. Lett. **106**, 259 (1986).
[17] J. C. D. Brand and A. R. Hoy, Appl. Spectrosc. Rev. **23**, 285 (1987).
[18] T. Ishiwata, S. Motohiro, E. Kagi, H. Fujiwara, and M. Fukushima, Bull. Chem. Soc. Jpn. **73**, 2255 (2000).
[19] J. C. D. Brand, A. R. Hoy, A. K. Kalker, and A. B. Yamashita, J. Mol. Spectrosc. **95**, 350 (1982).
[20] T. Ishiwata and I. Tanaka, Laser Chem. **7**, 79 (1987).
[21] M. L. Nowlin and M. C. Heaven, Chem. Phys. Lett. **239**, 1 (1995).
[22] J. P. Perot, M. Broyer, J. Chevalyre, and B. Femelat, J. Mol. Spectrosc. **98**, 161 (1983).
[23] X. Zheng, S. Fei, M. C. Heaven, and J. Tellinghuisen, J. Chem. Phys. **96**, 4877 (1992).
[24] H. Hemmati and G. J. Collins, Chem. Phys. Lett. **75**, 488 (1980).
[25] M. Martin, C. Fotakis, R. J. Donovan, and M. J. Shaw, Nuovo Cimento Soc. Ital. Fis., B **63**, 300 (1981).
[26] A. L. Guy, K. S. Viswanathan, A. Sur, and J. Tellinghuisen, Chem. Phys. Lett. **73**, 582 (1980).
[27] A. Kvaran, S. O. Jonsdottir, and T. E. Thorgeirsson, Proc.-Indian Acad. Sci., Chem. Sci. **103**, 417 (1991).
[28] M. J. Shaw, C. B. Edwards, F. O'Neill, C. Fotakis, and R. J. Donovan, Appl. Phys. Lett. **37**, 346 (1980).
[29] T. A. Stephenson, Y. Hong, and M. I. Lester, J. Chem. Phys. **94**, 4171 (1991); T. A. Stephenson, Y. Hong, and M. I. Lester, Chem. Phys. Lett. **159**, 549 (1989); T. A. Stephenson, Y. Hong, and M. I. Lester, in *Dynamics of Polyatomic van der Waals Complexes*, edited by N. Halberstadt and K. C. Janda (Plenum, New York, 1990), pp. 493–501.
[30] R. Teule, S. Stolte, and W. Ubachs, Laser Chem. **18**, 111 (1999).
[31] M. E. Akopyan, N. K. Bibinov, D. B. Kokh, A. M. Pravilov, O. L. Sharova, and M. B. Stepanov, Chem. Phys. **263**, 459 (2001).
[32] C. J. Fecko, M. A. Freedman, and T. A. Stephenson, J. Chem. Phys. **115**, 4132 (2001).
[33] R. J. LeRoy, University of Waterloo Chemical Physics Research Report, No. CP-230R3, 1986.
[34] D. R. T. Appadoo, R. J. Le Roy, P. F. Bernath, S. Gerstenkom, P. Luc, J. Vergès, J. Sinzelle, J. Chevillard, and Y. D'Aignaux, J. Chem. Phys. **104**, 903 (1996).
[35] D. Cerny, R. Bacis, S. Churassy, D. Inard, M. Lamrini, and M. Nota, Chem. Phys. **216**, 207 (1997).
[36] F. Martin, R. Bacis, S. Churassy, and J. Vergès, J. Mol. Spectrosc. **116**, 71 (1986).
[37] D. Inard, D. Cerny, M. Nota, R. Bacis, S. Churassy, and V. Skorokhodov, Chem. Phys. **243**, 305 (1999).
[38] T. A. Brunner and D. Pritchard, Adv. Chem. Phys. **50**, 589 (1982).
[39] K. Lawley, P. Jewsbury, T. Ridley, P. Langridge-Smith, and R. Donovan, Mol. Phys. **75**, 811 (1992).
[40] K. Yamasaki and S. R. Leone, J. Chem. Phys. **90**, 964 (1989).
[41] T. Ishiwata, H. Ohtoshi, M. Sakaki, and I. Tanaka, J. Chem. Phys. **80**, 1411 (1984).
[42] P. J. Dagdigian, D. Patel-Misra, A. Berning, H.-J. Werner, and M. H. Alexander, J. Chem. Phys. **98**, 8580 (1993).
[43] Ch. Ottinger, A. F. Vilesov, and D. D. Xu, J. Phys. Chem. **99**, 15642 (1995).
[44] R. Bachmann, X. Li, Ch. Ottinger, and A. F. Vilesov, J. Chem. Phys. **96**, 5151 (1992).
[45] R. Bachmann, X. Li, Ch. Ottinger, A. F. Vilsov, and V. Wulfmeyer, J. Chem. Phys. **98**, 8606 (1993).